Topologycal sensitivity analysis method: Theory and Applications

Maatoug Hassine

UR Analyse et Contrôle des EDP, FSM - Université de Monastir

Workshop on PDE's : Modelling and Theory
May 9-10, Monastir 2018

Model problem:

Find the optimal domain solution to

$$\min_{\Omega \in \mathcal{E}} j(\Omega)$$

where

- $j(\Omega) = J(\Omega, u_\Omega)$,
- u_Ω is the solution to a PDE defined in Ω,
- $\mathcal{E}$ is the set of admissible domains.

Topological Sensitivity analysis

Main idea : studying the variation of the design function j with respect to the creation of a small hole $\omega_{z,\varepsilon} = z + \varepsilon\omega$ at the point $z \in \Omega$, $\omega \subset \mathbb{R}^d$ fixed domain.

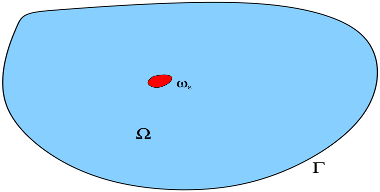

It leads to an asymptotic expansion of the form

$$j(\Omega \backslash \overline{\omega_{z,\varepsilon}}) - j(\Omega) = f(\varepsilon)\delta j(z) + o(f(\varepsilon)).$$

where

- $f(\varepsilon)$: is a scalar function known explicitly and goes to zero with ε $\lim_{\varepsilon \to 0} f(\varepsilon) = 0$.
- δj: topological gradient, called also topological sensitivity.

In order to minimize the cost function, the best location to insert a small hole in Ω is where δj is most negative.

In fact if $\delta j(z) < 0$, we have $j(\Omega \backslash \overline{\omega_{z,\varepsilon}}) < j(\Omega)$ for small ε.

In practice :

The optimal domain : It is obtained through insertion of some holes in the initial one

$$\mathcal{O}_{opt} = \Omega \backslash \overline{\cup_{k=1}^{m} \omega_k}$$

We build a sequence of geometries $\{\Omega_k\}_{k\geq 0}$ with $\Omega_0 = \Omega$.

The new geometry Ω_{k+1} is obtained by inserting some holes ω_k in Ω_k; $\Omega_{k+1} = \Omega_k \backslash \overline{\omega_k}$:

- The location of ω_k is given by the local minima of the topological gradient δj
- The shape of ω_k is defined by a level set curve of δj

$$\omega_k = \{x \in \Omega_k, \text{ such that } \delta j(x) \leq c_k < 0\},$$

where c_k is chosen in such a way that the cost function j decreases as most as possible.

History :

• It is introduced by Schumacher [1995] as "numerical approach" in structural mechanics using circular holes and Neumann b.c.

• Sokolowski [1999]: extended this idea to more general function using the adjoint method (case circular holes and Neumann b.c.).

• Masmoudi [2001]: introduced the Dirichlet condition case and given a more general approach to compute the topological gradient.

The topological sensitivity analysis has been derived for different linear operators: Elasticity, Laplace, Stokes, Helmholtz, Maxwell, ...

Recently, we have extended the mathematical analysis for Navier-Stokes operator.

Outline

1. Topological sensitivity analysis for the Stokes and Navier-Stokes operators w.r.t. the presence of a Dirichlet geometric perturbation
2. Applications :
   - Dynamic aeration process.
   - Geometric control problem.
   - Optimal shape design of tubes in a cavity.
3. Topological sensitivity analysis for the Stokes system with Neumann condition
4. Application : Detection of small flaws locations in moulded objects.
5. Conclusion

The Stokes system with Dirichlet condition:

In the perturbed domain $\Omega\backslash\overline{\omega_{z,\varepsilon}}$,
the velocity u_ε and the pressure p_ε satisfy

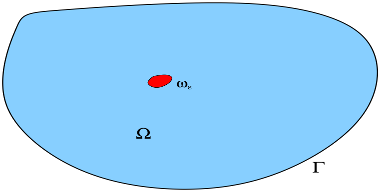

$$\begin{cases} -\operatorname{div}\,(2\nu\mathcal{D}(u_\varepsilon)) + \nabla p_\varepsilon &= \mathcal{G} \quad \text{in } \Omega\backslash\overline{\omega_{z,\varepsilon}} \\ \operatorname{div}\, u_\varepsilon &= 0 \quad \text{in } \Omega\backslash\overline{\omega_{z,\varepsilon}} \\ u_\varepsilon &= 0 \quad \text{on } \Gamma_d \\ (2\nu\mathcal{D}(u_\varepsilon) - p_\varepsilon I)\mathbf{n} &= g_n \quad \text{on } \Gamma_n \\ u_\varepsilon &= 0 \quad \text{on } \partial\omega_{z,\varepsilon} \text{ Dirichlet condition} \end{cases}$$

where $\mathcal{D}(u) = 1/2(\nabla u + \nabla u^T)$ is the rate of deformation tensor, ν is the fluid viscosity, $\mathcal{G}$ is a given body force and g_n is a given boundary datum.

Asymptotic expansion:

Let j be the design function

$$j(\Omega\backslash\overline{\omega_{z,\varepsilon}}) = J_\varepsilon(u_\varepsilon),$$

where J_ε is defined on $H^1(\Omega\backslash\overline{\omega_{z,\varepsilon}})$ verifying the following assumption $\mathcal{H}$:

1. J_0 is differentiable with respect to u, its derivative being denoted by $DJ_0(u)$.
2. There exists a real number δJ and a scalar function $f : \mathbb{R}_+ \longrightarrow \mathbb{R}_+$ such that $\forall\, \varepsilon \geq 0, \quad J_\varepsilon(u_\varepsilon) - J_0(u_0) = DJ_0(u_0)(u_\varepsilon - u_0) + f(\varepsilon)\delta J + o(f(\varepsilon)).$

Remark: We need to distinguish: $d = 2$ and $d = 3$.
If $d = 3$, the fundamental solution to the Stokes equations is given by

$$U(y) = \frac{1}{8\pi\nu r}\Big(I + e_r e_r^T\Big),\ P(y) = \frac{y}{4\pi r^3},\ \text{with } r = ||y||,\ e_r = y/r.$$

If $d = 2$, The fundamental solution to the Stokes equations is given by

$$U(y) = \frac{1}{4\pi\nu}\Big(-\log(r)I + e_r e_r^T\Big),\ P(y) = \frac{y}{2\pi r^2}.$$

Theorem: 3D case

If the assumption $\mathcal{H}$ holds, the function j has the asymptotic expansion

$$j(\Omega\backslash\overline{\omega_{z,\varepsilon}}) - j(\Omega) = \varepsilon\left[\left(-\int_{\partial\omega}\eta(y)\ \mathrm{ds(y)}\right).v_0(z) + \delta J\right] + o(\varepsilon).$$

- v_0 is the solution to the associated adjoint problem in Ω.
- $\eta \in H^{-1/2}(\partial\omega)^d$ is solution to the next boundary integral equation,

$$\int_{\partial\omega} U(x-y)\,\eta(y)\ ds(y) = -u_0(z), \quad \forall x \in \partial\omega.$$

- u_0 is the solution to the Stokes equations in Ω.

3D - Spherical case:

In the particular case where $\omega = B(0,1)$, the density η is given by $\eta(y) = -\dfrac{3\nu}{2} u_0(z),\ \forall y \in \partial\omega.$

Theorem: 3D - spherical case

If $\omega = B(0,1)$, under the assumption $\mathcal{H}$, we have

$$j(\Omega \backslash \overline{\omega_{z,\varepsilon}}) - j(\Omega) = \varepsilon \left[6\pi\nu\, u_0(z).v_0(z) + \delta J \right] + o(\varepsilon).$$

2D case:

Theorem: 2D case

If the assumption $\mathcal{H}$ holds, the function j has the asymptotic expansion

$$j(\Omega \backslash \overline{\omega_{z,\varepsilon}}) - j(\Omega) = \frac{-1}{\log(\varepsilon)} \left[4\pi\nu\, u_0(z).v_0(z) + \delta J \right] + o\left(\frac{-1}{\log(\varepsilon)} \right).$$

Topological sensitivity analysis for the Navier-Stokes operator

Theorem: 3D case

$$\| u_\varepsilon - u_0 - W \|_{L^2(0,T;\,H^1(\Omega_{z,\,\varepsilon}))} \leq c\varepsilon,$$

where the leading term $W = (W^1, W^2, W^3) \in H^1(\Omega_{z,\,\varepsilon})^3$ is defined by

$$W^j(x,t) = U^j(\frac{x-z}{\varepsilon}).u_0(z,\,t),\ \forall (x,\,t) \in \mathbb{R}^3 \backslash \overline{\mathcal{O}_{z,\varepsilon}} \times]0,\ T[, \tag{1}$$

with U^j is solution to the following Stokes exterior problem

$$\left\{ \begin{array}{rlll} -\nu\Delta U^j + \nabla P^j & = 0 & \text{in} & \mathbb{R}^3\backslash\overline{\mathcal{O}}, \\ \operatorname{div} U^j & = 0 & \text{in} & \mathbb{R}^3\backslash\overline{\mathcal{O}}, \\ U^j & \longrightarrow 0 & \text{at} & \infty, \\ U^j & = -e_j & \text{on} & \partial\mathcal{O}. \end{array} \right. \tag{2}$$

Here $\{e_j\}_{j=1,2,3}$ is the canonical basis of $\mathbb{R}^3$.

Topological sensitivity analysis for the Navier-Stokes operator

Theorem: 3D case (M.H and R. Malek, 2017)

The shape function j satisfies the asymptotic expansion

$$j(\Omega \setminus \overline{\mathcal{O}_{z,\varepsilon}}) = j(\Omega) + \varepsilon \Big[\int_0^T w_0(z,\ t).\mathcal{M}_{\mathcal{O}} v_0(z,\ t)dt + \delta\mathcal{J} \Big] + o(\varepsilon), \qquad (3)$$

where

$-$ $\mathcal{M}_{\mathcal{O}}$ is the matrix defined by

$$\mathcal{M}_{\mathcal{O}ij} = \int_{\partial\mathcal{O}} \eta_i^j(y) ds(y),\ 1 \le i, j \le 3.$$

$-$ v_0 is the solution to the following associated adjoint problem

Topological sensitivity analysis for the Navier-Stokes operator

Theorem: 2D case

$$\| u_\varepsilon - u_0 - W \|_{L^2(0,T;\, H^1(\Omega\backslash\overline{\omega_{z,\varepsilon}}))} \leq \frac{-c}{\log(\varepsilon)}$$

where $W(x,t) = \dfrac{4\pi\nu}{\log(\varepsilon)} U(x-z)\, u_0(z,\ t), \quad \forall (x,\ t) \in \Omega\backslash\overline{\omega_{z,\varepsilon}} \times]0,\ T[.$

The asymptotic expansion :

Theorem: 2D case (M.H and R. Malek, 2017)

$$j(\Omega\backslash\overline{\omega_{z,\varepsilon}}) = j(\Omega) + \frac{-1}{\log(\varepsilon)} \left[4\pi\nu \int_0^T u_0(z,\ t)\, v_0(z,\ t)\, dt + \delta\mathcal{J} \right] + o\left(\frac{-1}{\log(\varepsilon)} \right).$$

where v_0 is the solution to the associated adjoint problem

APPLICATIONS

- **Dynamic aeration process.**
- **Geometric control problem.**
- **Optimal shape design of tubes in a cavity.**

I - Dynamic aeration process

Eutrophication problem:

In arid and semi-arid areas (high temperature, a neglected wind effect), the thermic factors combined to the biological and to the chemical ones generate a stratification process.

Main chacarterization: a poor dissolved oxygen concentration in water.
$\Longrightarrow$ that decrease of the water quality.

Proposed solution: the dynamic aeration process.

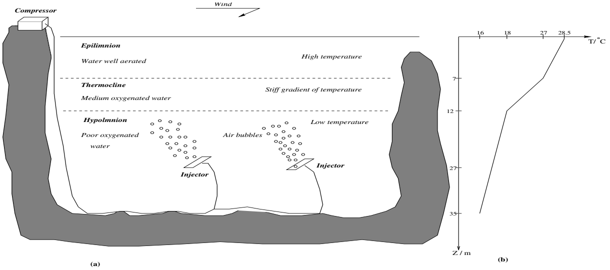

(a): Structure of a stratified lake, (b): average temperature curve during summer.

Goal: oxygenation of the water.
Idea: generate a vertical motion mixing up the water of the bottom with that in the top.
Tools: inserting air by the means of injectors located in the bottom of the lake.

Optimization of injectors location.

Aim: Generate the best motion in the fluid with respect to the aeration purpose.

Model:

- The fluid flow is governed by the Quasi-Stokes equations.
- Each injector Inj_k is modeled as a small hole $\omega_{z_k,\varepsilon} = z_k + \varepsilon\omega^k$, $1 \leq k \leq m$ having an injection velocity u_{inj}^k.
- The velocity u_ε and the pressure p_ε satisfy

$$\begin{cases} \alpha u_\varepsilon - \nu\Delta u_\varepsilon + \nabla p_\varepsilon &= F \quad \text{in } \Omega\backslash\cup_{k=1}^m \overline{\omega_{z_k,\varepsilon}} \\ \nabla . u_\varepsilon &= 0 \quad \text{in } \Omega\backslash\cup_{k=1}^m \overline{\omega_{z_k,\varepsilon}} \\ u_\varepsilon &= u_d \quad \text{on } \Gamma \\ u_\varepsilon &= u_{inj}^k \quad \text{on } \cup_{k=1}^m \partial\omega_{z_k,\varepsilon}, \end{cases}$$

where ν is the fluid viscosity, F is a given body force, u_d is a given boundary velocity and u_{inj}^k is a given injection velocity on $\partial\omega_{z_k,\varepsilon}$, $1 \leq k \leq m$.

Criterion: we assume that a "good" lake aeration can be described by a target velocity $\mathcal{U}_g$.
The cost function J_ε to be minimized is defined by

$$J_\varepsilon(u_\varepsilon) = \int_{\Omega_m} |u_\varepsilon - \mathcal{U}_g|^2 \, dx,$$

where u_ε is the velocity field solution to the Quasi-Stokes equations and $\Omega_m \subset \Omega$ is the measurement domain (the top layer).

The identification problem can be formulated as:

Topological optimization problem:

$$\min_{\omega_{z_k,\varepsilon} \subset \Omega} j(\Omega \setminus \cup_{k=1}^{m} \overline{\omega_{z_k,\varepsilon}}),$$

where j is the design function defined by

$$j(\Omega \setminus \cup_{k=1}^{m} \overline{\omega_{z_k,\varepsilon}}) = J_\varepsilon(u_\varepsilon),$$

Injectors location:

The algorithm:

- Initialization: choose $\Omega_0 = \Omega$, and set $k = 0$.
- Repeat until target is reached:
  - solve the direct and the adjoint problems in Ω_k,
  - compute the topological sensitivity δj_k,
  - determine the set $H_k = \{x \in \Omega_k; \quad \delta j_k(x) < c_k < 0\}$, where c_k is chosen in such a way that the cost function decreases,
  - set $\Omega_{k+1} = \Omega_k \backslash H_k$,
- $k \longleftarrow k + 1$.

At the k^{th} iteration, the topological gradient δj_k is given by

$$\delta j_k(z) = \left(u_k(x) - u_{inj}\right).v_k(x), \quad \forall z \in \Omega_k$$

where u_k and v_k are, respectively, solution to the direct and adjoint problems in Ω_k.

Numerical results:

Initial flow

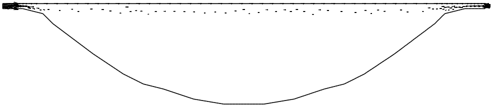

Objective flow

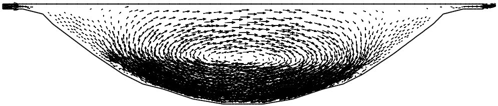

Obtained flow

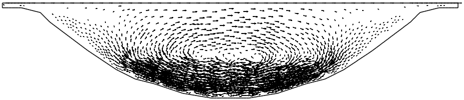

Obtained injectors locations

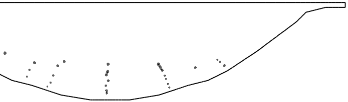

Dynamic aeration process

3D case : Numerical simulation of the aeration process

The lake geometry

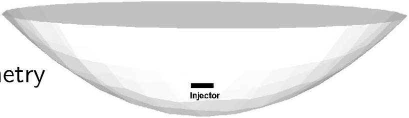

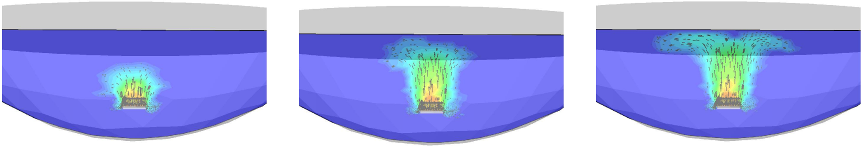

Velocity field: at time 1s, 1mn and 10mn

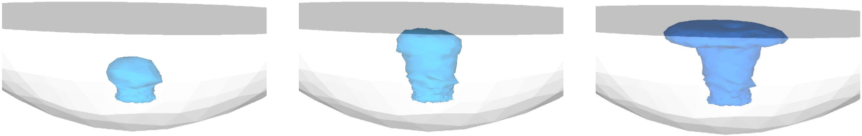

Aerated zone: at time 1s, 1mn and 10mn

3D case: Optimization of injectors location

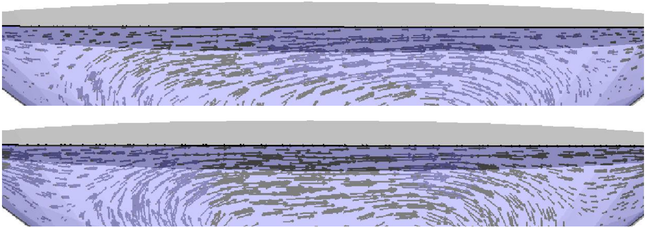

The wanted (top) and obtained (bottom) velocities in Ω_m

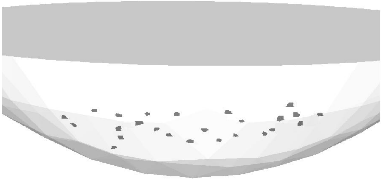

Obtained injectors locations

II - Geometric control of fluid flow

We consider an incompressible fluid in a cavity Ω, having some inlets Γ^i_{in}, $1 \leq i \leq n$, and some outlets Γ^j_{out}, $1 \leq j \leq m$.

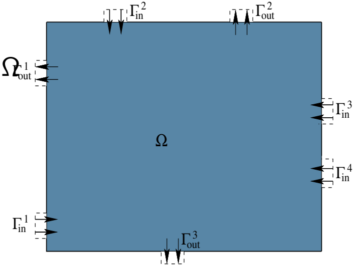

Goal : Determine the optimal shape $\mathcal{O}^*$ solution to

$$\min_{\mathcal{O}\subset\Omega} \int_{\Omega_m} |u_{\mathcal{O}} - w_{obj}|^2 dx,$$

where w_{obj} is a wanted velocity field defined in a fixed zone Ω_m.

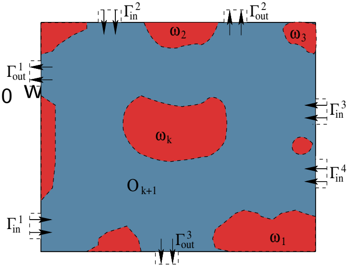

Idea: build a sequence of geometries $(\Omega_k)_{k\geq 0}$ w
$\Omega_{k+1} = \Omega_k \backslash \overline{\omega_k}$. .

$\Longrightarrow$ ω_k is solution to

$$\min_{\omega_k \subset \mathcal{O}_k} j(\mathcal{O}_k \backslash \overline{\omega_k}),$$

Topological sensitivity method : The obstacle ω_k is defined by a level set curve of δj_k

$$\omega_k = \{x \in \Omega_k, \text{ such that } \delta j_k(x) \leq c_k < 0\},$$

where c_k is chosen in such a way that j decreases as much as possible.

The algorithm:

- Initialization: choose $\Omega_0 = \Omega$, and set $k = 0$.
- Repeat until $\delta j_k \geq 0$ in Ω_k:
  - solve the Stokes equations in Ω_k,
  - solve the associated adjoint problem in Ω_k,
  - compute the topological sensitivity $\delta j_k(x)\ \forall x \in \Omega_k$,
  - determine the obstacle ω_k,
  - set $\Omega_{k+1} = \Omega_k \backslash \overline{\omega_k}$,
- $k \longleftarrow k+1$.

- **Test 1:** Optimization of a purification tank through insertion of obstacles.

$$\min_{\mathcal{O}\subset\Omega} \int_{\Omega_m} |u_{\mathcal{O}} - w_d|^2 dx,$$

where $u_{\mathcal{O}}$ is the solution to the Stokes equations in $\mathcal{O} \subset \Omega$.

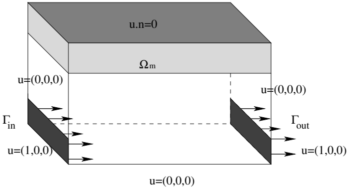

The initial geometry

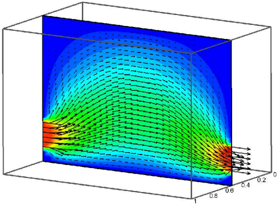

The initial velocity field

- **Numerical results:** The optimal domain is obtained in only 5 iterations.

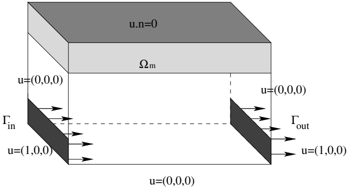

The optimal domain

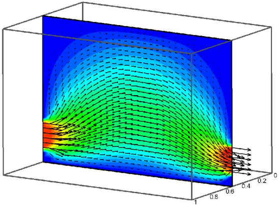

The final velocity field

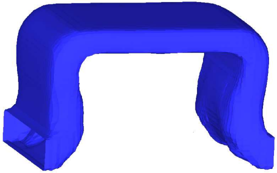

The optimal domain

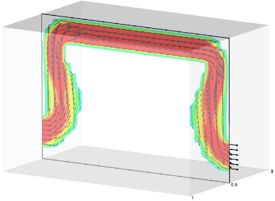

The final velocity field

- **Numerical results**

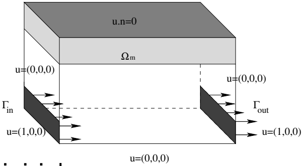

initial geometry

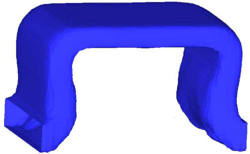

obtened geometry

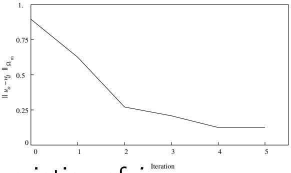

variation of j

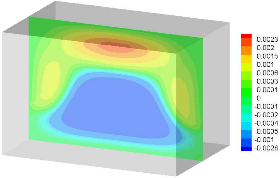

iteration 1

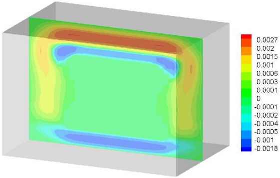

iteration 3

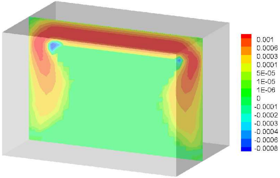

iteration 5

The topological gradient

- **Test 2:** Maximize the fluid flow velocity in $\Omega_m = \cup_k \Omega_m^k \subset \Omega$.

$$\max_{\mathcal{O}\subset\Omega} \int_{\Omega_m} |u_{\mathcal{O}}|^2 dx,$$

where $u_{\mathcal{O}}$ is the solution to the Stokes equations in $\mathcal{O}$.

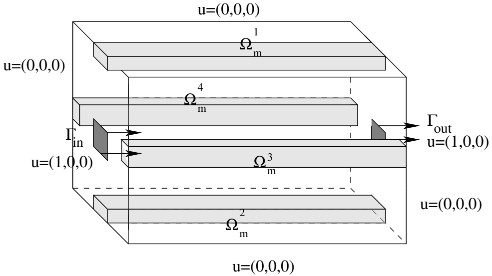

The initial geometry and the fixed domain Ω_m

- **Numerical results:** The optimal domain is obtained in only 5 iterations.

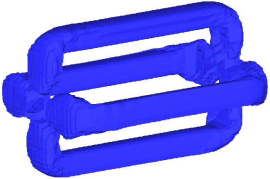

The optimal domain

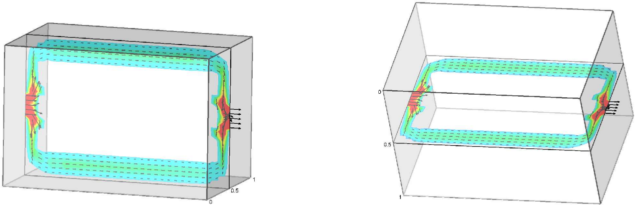

2D cuts of the final velocity field

III - Optimal shape design of tubes in a cavity

We consider an incompressible fluid in a cavity Ω having one inlet and some outlets.

Goal: Determine the optimal shape of the tubes that connect the inlet to the outlets of the cavity minimizing the dissipated power in the fluid.

$$\min_{\mathcal{O}\subset\Omega} \int_{\mathcal{O}} |\nabla u_{\mathcal{O}}|^2 \mathrm{dx},$$

with

- $u_{\mathcal{O}}$ is the solution to Navier-Stokes equations in $\mathcal{O}$.
- $meas(\mathcal{O}) = V_0$

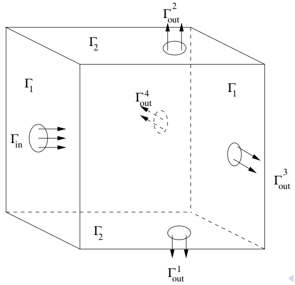

- **Test 1:** One inlet, two outlets.

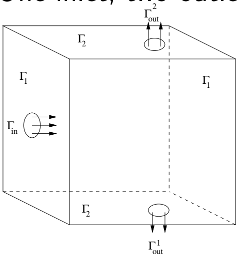

The initial geometry

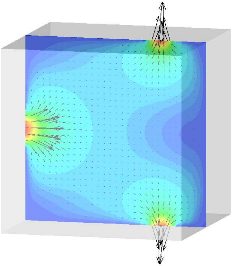

2D cut of the initial velocity field

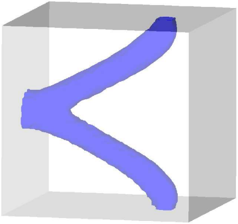

The optimal domain

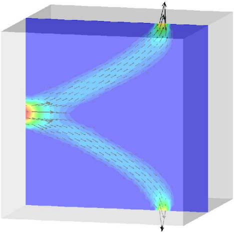

The obtained velocity field

Optimal shape design

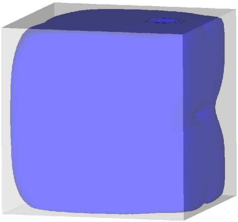

iteration 1

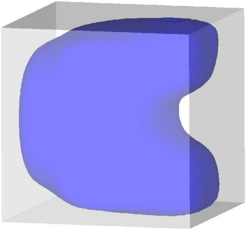

iteration 3

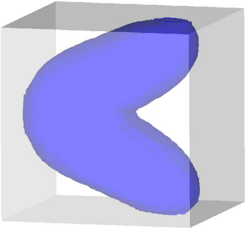

iteration 5

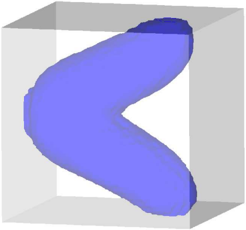

iteration 8

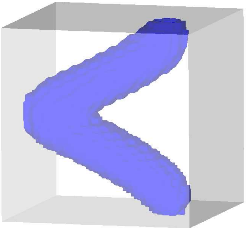

iteration 10

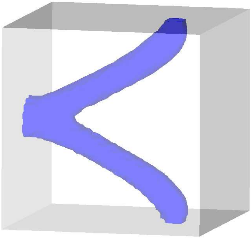

iteration 12

Optimal shape design

- **Test 2:** One inlet, four outlets.

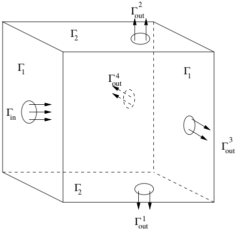

The initial geometry

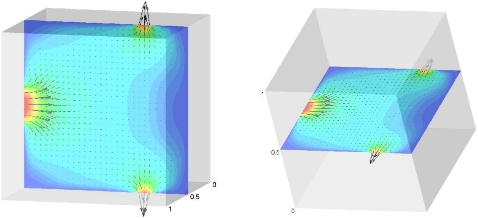

2D cut of the initial velocity field

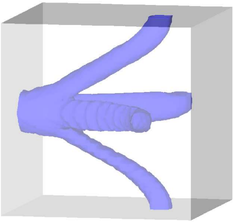

The optimal domain

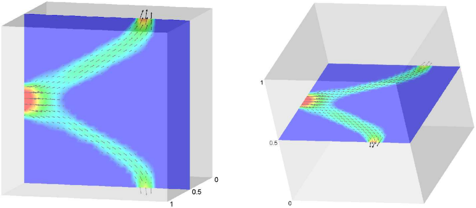

The obtained velocity field

Optimal shape design

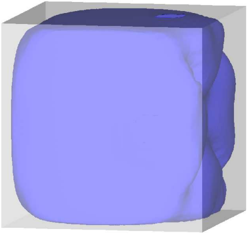

iteration 2

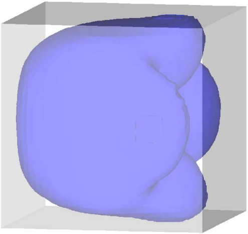

iteration 4

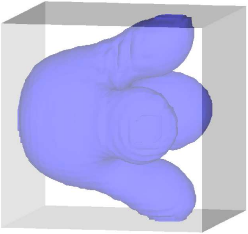

iteration 6

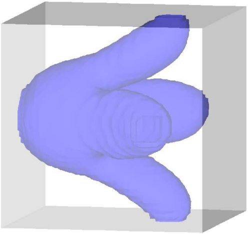

iteration 9

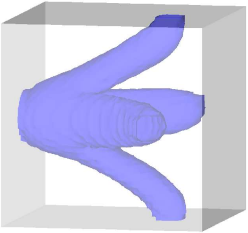

iteration 13

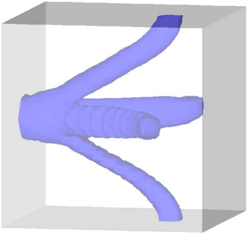

iteration 16

Detection of small flaws locations in moulded objects

The Mould filling process: The mould filling is an industrial process used in fabrication of the metal pieces.

The mould filling process is based on the two phases:

- The Mould filling phase: simulation of the liquid/air interface.
- The solidification phase: simulation of the solid/liquid interface.

$\Longrightarrow$ numerical simulation of two free surfaces.

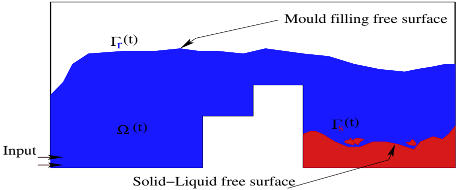

Mould filling process

Model : based on the Navier-Stokes system and the energie equation.

Maronnier V., Picasso M., Rappaz J. (1999) and (2003)

Creation of bubbles of gas : During the mould filling process, gas bubbles may be trapped by the fluid and cannot escape.

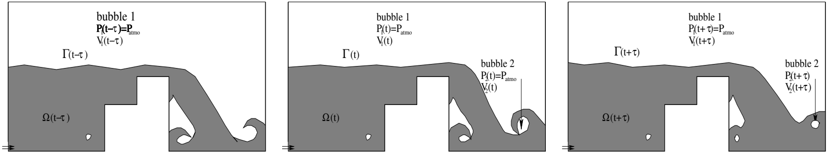

Creation of bubbles of gas during the mould filling process

Some numerical simulations and experimental results showing the creation of bubbles of gas are given in

Caboussat A., Picasso M., Rappaz J.(2005), *Numerical simulation of free surface incompressible liquid flows surrounded by compressible gas*, J. Comput. Physics, **203**, 626-649.

Direct problem : numerical simulation of the fluid flow in the presence of some bubbles of gas.

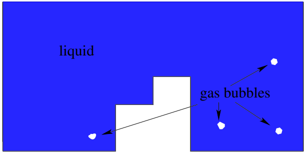

Fluid flow model:

- After the filling phase the fluid flow can be characterized by a low velocity or a high viscosity (i.e. low Reynold number). The Stokes equations can be used as an approximation of the full Navier-Stokes equations.
- an homogeneous Neumann boundary condition on the liquid-gas interface.

For a given force g acting on Γ, the velocity U_ε and the pressure P_ε satisfy

$$\left\{\begin{array}{rcl} -\operatorname{div}\left(2\nu\mathcal{D}(U_\varepsilon)\right)+\nabla P_\varepsilon = & \mathcal{G} & \text{in } \Omega\backslash\overline{\omega_\varepsilon} \\ \operatorname{div} U_\varepsilon = & 0 & \text{in } \Omega\backslash\overline{\omega_\varepsilon} \\ (2\nu\mathcal{D}(U_\varepsilon)-P_\varepsilon I)\mathbf{n} = & g & \text{on } \Gamma \\ (2\nu\mathcal{D}(U_\varepsilon)-P_\varepsilon I)\mathbf{n} = & 0 & \text{on } \partial\omega_\varepsilon, \end{array}\right.$$

where ω_ε is the domain occupied by the gas.

The inverse problem : detect the gas bubbles locations from boundary measurement of velocities.

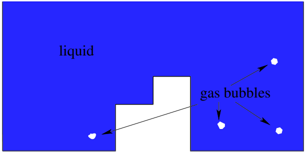

Assumptions :

- Each bubble of gas is modelled as a small hole having geometry form $\omega_{z_k,\varepsilon} = z_k + \varepsilon\omega^k$, $1 \le k \le m$, where ε is the shared diameter and $\omega^k \subset \mathbb{R}^d$ are bounded and smooth domains containing the origin.
- The gas bubbles $\omega_{z_k,\varepsilon}$ are well separated.

The inverse problem :

Given : ◇ the prescribed boundary force g (acting on Γ),
◇ the measured velocity $\mathcal{U}_d$ on Γ.

Find : the gas bubbles locations in the mould Ω.

Misfit function: We use the over-specified boundary data.

For any set of bubbles $\omega_\varepsilon = \cup_{k=1}^m z_k + \varepsilon\omega^k \subset \Omega$ two forward problems.

Neumann problem: find $(u_{_N}^\varepsilon,\, p_{_N}^\varepsilon)$ solution to

$$\left\{\begin{array}{rl} -\operatorname{div}\left(2\nu\mathcal{D}(u_{_N}^\varepsilon)\right) + \nabla p_{_N}^\varepsilon = \mathcal{G} & \text{in } \Omega\backslash\overline{\omega_\varepsilon} \\ \operatorname{div} u_{_N}^\varepsilon = 0 & \text{in } \Omega\backslash\overline{\omega_\varepsilon} \\ (2\nu\mathcal{D}(u_{_N}^\varepsilon) - p_{_N}^\varepsilon I)\mathbf{n} = g & \text{on } \Gamma \\ (2\nu\mathcal{D}(u_{_N}^\varepsilon) - p_{_N}^\varepsilon I)\mathbf{n} = 0 & \text{on } \partial\omega_\varepsilon. \end{array}\right.$$

Dirichlet problem: find $(u_{_D}^\varepsilon,\, p_{_D}^\varepsilon)$ solution to

$$\left\{\begin{array}{rl} -\operatorname{div}\left(2\nu\mathcal{D}(u_{_D}^\varepsilon)\right) + \nabla p_{_D}^\varepsilon = \mathcal{G} & \text{in } \Omega\backslash\overline{\omega_\varepsilon} \\ \operatorname{div} u_{_D}^\varepsilon = 0 & \text{in } \Omega\backslash\overline{\omega_\varepsilon} \\ u_{_D}^\varepsilon = \mathcal{U}_d & \text{on } \Gamma \\ (2\nu\mathcal{D}(u_{_D}^\varepsilon) - p_{_D}^\varepsilon I)\mathbf{n} = 0 & \text{on } \partial\omega_\varepsilon. \end{array}\right.$$

Misfit function:

The actual domain of gas is obtained $(\omega_\varepsilon = \omega^*)$ when the misfit between the solutions vanishes, $u_D^\varepsilon = u_N^\varepsilon$.

$\Downarrow$

The Kohn-Vogelius function :

$$\mathcal{E}_\varepsilon(u_N^\varepsilon, u_D^\varepsilon) = 2\nu \left\| \mathcal{D}(u_N^\varepsilon) - \mathcal{D}(u_D^\varepsilon) \right\|^2_{L^2(\Omega \setminus \overline{\omega_\varepsilon})}.$$

Such a function has two main features:

- It is an energy function $\Longrightarrow$ we don't need an additional regularization to stabilize the recovery process.
- We don't need to compute the adjoint state.

The inverse problem:

Given the boundary force g and the measured velocity $\mathcal{U}_d$:
Find the optimal location z_k^* of the gas bubbles $\omega_{z_k,\varepsilon} = z_k + \varepsilon\omega^k,\ 1 \leq k \leq m$ solution to

$$\min_{z_k \in \Omega} \mathcal{E}_\varepsilon(u_N^\varepsilon, u_D^\varepsilon),$$

Modelling each gas bubble $\omega_{z_k,\varepsilon}$ as a small hole centred at z_k, the inverse problem is turned in a topological optimization one.

Topological optimization problem:

$$\min_{\omega_{z_k,\varepsilon} \in \Omega} \mathcal{J}(\Omega \backslash \overline{\omega_\varepsilon}),$$

where $\mathcal{J}$ is a design function defined by $\mathcal{J}(\Omega \backslash \overline{\omega_\varepsilon}) = \mathcal{E}_\varepsilon(u_N^\varepsilon, u_D^\varepsilon)$ and $\omega_\varepsilon = \cup_{k=1}^m z_k + \varepsilon\omega^k$.

Tools : we shall use the **topological gradient method**.

The Stokes system with Neumann condition:

In the perturbed domain $\Omega \backslash \overline{\omega_{z,\varepsilon}}$,
the velocity u_ε and the pressure p_ε satisfy

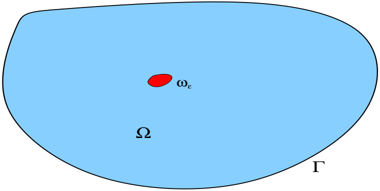

$$\begin{cases} -\operatorname{div}\,(2\nu\mathcal{D}(u_\varepsilon)) + \nabla p_\varepsilon & = \mathcal{G} & \text{in } \Omega\backslash\overline{\omega_{z,\varepsilon}} \\ \operatorname{div}\, u_\varepsilon & = 0 & \text{in } \Omega\backslash\overline{\omega_{z,\varepsilon}} \\ u_\varepsilon & = 0 & \text{on } \Gamma_d \\ (2\nu\mathcal{D}(u_\varepsilon) - p_\varepsilon I)\mathbf{n} & = g_n & \text{on } \Gamma_n \\ (2\nu\mathcal{D}(u_\varepsilon) - p_\varepsilon I)\mathbf{n} & = 0 & \text{on } \partial\omega_{z,\varepsilon} \text{ Neumann condition} \end{cases}$$

where $\mathcal{D}(u) = 1/2(\nabla u + \nabla u^T)$ is the rate of deformation tensor and I is the $d \times d$ identity matrix.

Assumption $\mathcal{H}$:

- J_ε is differentiable with respect to u, its derivative being denoted by $DJ_\varepsilon(u)$.
- There exist a real number δJ and a real function $f : \mathbb{R}_+ \longrightarrow \mathbb{R}_+$ such that

$$J_\varepsilon(u_\varepsilon) - J_0(u_0) = DJ_\varepsilon(u_\varepsilon - u_0) + f(\varepsilon)\delta J + \circ(f(\varepsilon)),$$
$$\lim_{\varepsilon \to 0} f(\varepsilon) = 0.$$

- The associated adjoint problem has a unique solution.

Main results : we have derived a topological Sensitivity analysis valid for

- large class of cost function,
- arbitrary shaped holes

Theorem : "general case"

If the cost function J_ε satisfies the assumptions $\mathcal{H}$, then j has the following asymptotic expansion

$$j(\Omega \backslash \overline{\omega_{z,\varepsilon}}) = j(\Omega) + \varepsilon^d \Big(-\mathcal{D}(u_0)(z) : \mathcal{M}\mathcal{D}(v_0)(z) + |\omega|\, \mathcal{G}\, v_0(z) + \delta J \Big) + o(\varepsilon^d),$$

where

- u_0 solution to the Stokes equations in Ω,
- v_0 solution to the associated adjoint problem,
- $\mathcal{M}$ is the Viscous Moment Tensor associated to the domain ω and the viscosity ν.

The Viscous Moment Tensor: The Viscous Moment Tensor $\mathcal{M}$ is given by

$$\mathcal{M}_{ij}^{pq} = 2\nu \int_{\partial\omega} y_i \, \eta_j^{p,q}(y) \, \mathrm{ds}, \forall 1 \leq i, j, p, q \leq d$$

where y_i denotes the i^{th} component of $y \in \mathbb{R}^d$, and $\eta^{p,q} \in H^{-1/2}(\partial\omega)^d$ is the solution to:

$$-\frac{\eta^{p,q}(y)}{2} + \int_{\partial\omega} [(2\nu \mathcal{D}_y(E)(x-y)\eta^{p,q}(x))\mathbf{n}(y) - P(x-y)\eta^{p,q}(x)\mathbf{n}(y)] \, \mathrm{ds} = -\mathcal{I}^{p,q}\mathbf{n}(y) \;\; \forall y \in \partial\omega,$$

with $\mathcal{I}^{p,q} \in \mathbb{R}^d \times \mathbb{R}^d$, $1 \leq p, q \leq d$ is the symmetric matrix defined by

$$\mathcal{I}_{ij}^{pq} = \frac{1}{2}(\delta_{ip}\delta_{jq} + \delta_{iq}\delta_{jp}), \; \forall 1 \leq i, j \leq d.$$

Here δ_{kl} denotes the Kronecker symbol.

Properties of the Viscous Moment Tensor:

Proposition :

The Viscous Moment Tensor $\mathcal{M}$ is positive definite

Proposition :

The Viscous Moment Tensor $\mathcal{M}$ is symmetric in the following sens

$$\mathcal{M}_{ij}^{pq} = \mathcal{M}_{ij}^{qp}, \quad \mathcal{M}_{ij}^{pq} = \mathcal{M}_{ji}^{pq}, \text{ and } \mathcal{M}_{ij}^{pq} = \mathcal{M}_{pq}^{ij}, \quad \forall\, p,\, q,\, k,\, l \in \{1, ..., d\}.$$

If $\omega = B(0,1)$ the integral equation has an explicit solution

$$\eta(y) = \begin{cases} 4\nu\mathcal{D}(v_0)y, & \forall y \in \partial\omega \quad \text{if } d = 2, \\ 3\nu\mathcal{D}(v_0)y, & \forall y \in \partial\omega \quad \text{if } d = 3. \end{cases}$$

Then, the tensor $\mathcal{M}$ is given by

$$\mathcal{M} = 4\pi\nu\mathcal{I} \quad \text{if } d = 2 \text{ or } 3,$$

where $\mathcal{I}$ is the $d^2 \times d^2$ identity matrix.

Corollary: "spherical case"

If $\omega = B(0,1)$, j has the asymptotic expansion

$$j(\Omega\backslash\overline{\omega_{z,\varepsilon}}) - j(\Omega) = \pi\varepsilon^d \delta j(z) + o(\varepsilon^d).$$

where

$$\delta j(z) = \begin{cases} -4\nu\mathcal{D}(u_0)(z) : \mathcal{D}(v_0)(z) + \mathcal{G}\, v_0(z) + \delta J & \text{if } d = 2, \\ \\ -4\nu\mathcal{D}(u_0)(z) : \mathcal{D}(v_0)(z) + (4/3)\,\mathcal{G}\, v_0(z) + \delta J & \text{if } d = 3. \end{cases}$$

Cost function examples:

Proposition:

The cost function

$$J_\varepsilon(u) = \int_{\Omega \setminus \overline{\omega_{z,\varepsilon}}} |u|^2 \, \mathrm{dx}$$

satisfies the assumptions $\mathcal{H}_1$ and $\mathcal{H}_2$ with

- $\delta J = -|\omega| \, |u_0(z)|^2$, $z \in \Omega$
- $L_\varepsilon(w) = 2 \displaystyle\int_{\Omega \setminus \overline{\omega_{z,\varepsilon}}} u_0 \, w \, \mathrm{dx}$, $\forall w \in \mathcal{V}_\varepsilon$
- $L = 2u_0$.

Cost function examples:

Proposition:

The cost function

$$J_\varepsilon(u) = 2\nu \int_{\Omega\setminus\overline{\omega_{z,\varepsilon}}} |\mathcal{D}(u)|^2 \, \mathrm{dx},$$

satisfies the assumptions $\mathcal{H}_1$ and $\mathcal{H}_2$ with

- $\delta J = -\mathcal{D}(u_0)(z) : \mathcal{M}\mathcal{D}(u_0)(z), \; z \in \Omega$
- $L_\varepsilon(w) = 2\int_{\Omega\setminus\overline{\omega_{z,\varepsilon}}} \mathcal{G} w \mathrm{dx} + 2\int_{\Gamma_n} g_n w \mathrm{dx}, \forall w \in \mathcal{V}_\varepsilon$
- $L = 2\,\mathcal{G}$.

Sensitivity analysis for the misfit functional:

Theorem : "spherical shaped flaw"

If $\omega = B(0,1)$ we have

$$\mathcal{J}(\Omega_{z,\varepsilon}) - \mathcal{J}(\Omega) = \pi\varepsilon^d \delta\mathcal{J}(z) + o(\varepsilon^d),$$

with

- **2D case:**

$$\begin{aligned}\delta\mathcal{J}(z) = 4\nu[&\mathcal{D}(u_N^0)(z) : \mathcal{D}(u_N^0)(z) - \mathcal{D}(u_D^0)(z) : \mathcal{D}(u_D^0)(z)] \\ &+2\mathcal{G}\,[u_D^0(z) - u_N^0(z)]\end{aligned}$$

- **3D case:**

$$\begin{aligned}\delta\mathcal{J}(z) = 4\nu[&\mathcal{D}(u_N^0)(z) : \mathcal{D}(u_N^0)(z) - \mathcal{D}(u_D^0)(z) : \mathcal{D}(u_D^0)(z)] \\ &+(8/3)\,\mathcal{G}\,[u_D^0(z) - u_N^0(z)].\end{aligned}$$

The algorithms

- We consider the the bi-dimensional case.
- The topological gradient is given by :

$$\delta\mathcal{J}(z) = 4\nu[\mathcal{D}(u_N^0)(z) : \mathcal{D}(u_N^0)(z) - \mathcal{D}(u_D^0)(z) : \mathcal{D}(u_D^0)(z)] \\ +2\mathcal{G}\,[u_D^0(z) - u_N^0(z)].$$

- The measurements data $\mathcal{U}_d$ are synthetic.

One-shot algorithm:

- Solve the two direct problems: $(\mathcal{P}_N^0)$ and $(\mathcal{P}_D^0)$,
- Compute the topological gradient $\delta\mathcal{J}(z)$, $z \in \Omega$,
- Determine the negative local minima of $\delta\mathcal{J}(z)$.

Bubbles location: Bubbles are likely to be located at spots where the topological gradient δj is most negative.

Implementation:

- **Mould geometry:** The rectangular $\Omega = [0,1] \times [0,0.5]$ is used as a mould filled with a viscous and incompressible fluid.
- **Discretization:** The domain Ω is discretized by triangular mesh using a mesh step equal to h.

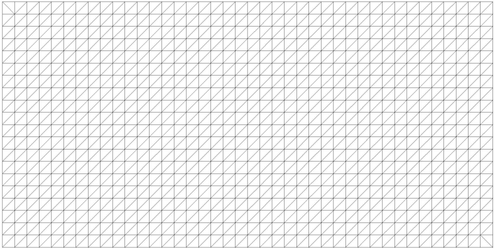

The domain Ω is discretized by triangular mesh

Detection of small flaws locations in moulded objects

Detection results: One bubble

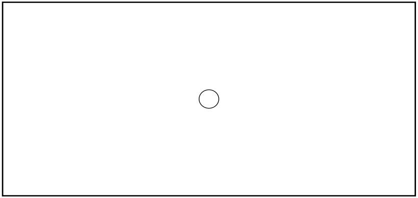

Exact location of $\omega^* = z^* + 0.01B(0,1)$

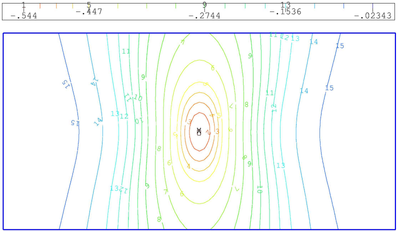

Isovalues of δj

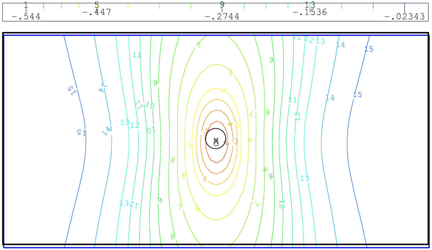

Detection results: three bubbles

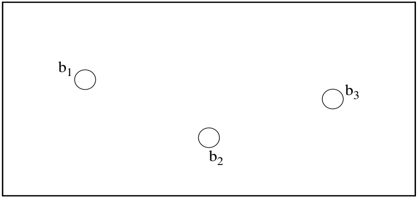

Exact locations

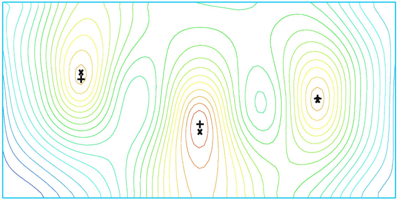

Isovalues of δj

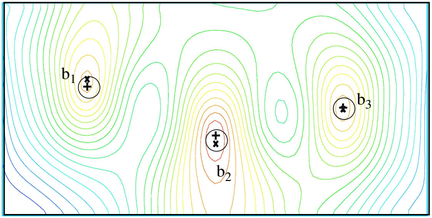

Detection results with noisy data:

We consider the case of three well-separated flaws having the same radius $r* = 0.02$, $b_1 = B(z_1^*, r*)$, $b_2 = B(z_2^*, r*)$ and $b_3 = B(z_3^*, r*)$.

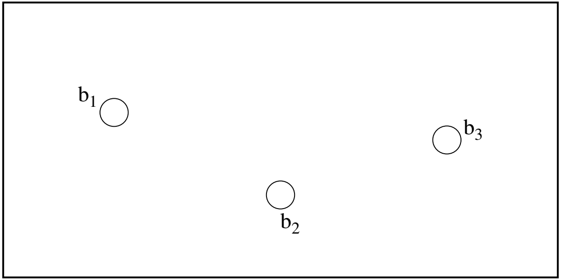

Figure: Mould containing three well-separated flaws having the same radius; $b_1 = B(z_1^*, r*)$, $b_2 = B(z_2^*, r*)$ and $b_3 = B(z_3^*, r*)$

The data $\mathcal{U}_d$ is polluted by a pointwise white noise with an amplitude ranging from 0 to 0.1.

Detection results with noisy data: The considered error function is given by

$$er(\tau) = \frac{1}{3}\sum_{k=1}^{3} \frac{\left\| z_h^k(\tau) - z_k^* \right\|}{2\, r*},$$

- τ is the noise level,
- z_h^k, $1 \leq k \leq 3$, are the computed flaw's center.

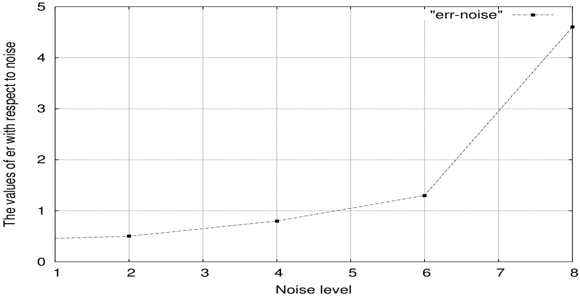

Figure: Variation of the error function with respect to the noise level τ; 0%, 2%, 4%, 6%, and 8%.

Detection results with noisy data:

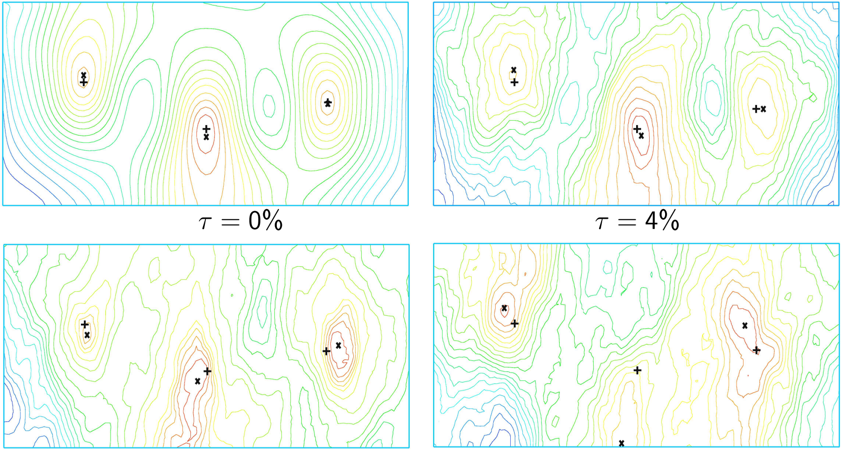

$\tau = 0\%$ $\tau = 4\%$

$\tau = 6\%$ $\tau = 8\%$

Figure: Isovalues of the topological gradient showing the flaw locations obtained using different level of noise($\times$: exact, o: estimated).

Limites of the One-shot algorithm:

- Sensitivity to the depth
- Sensitivity to the relative position of two flaws
- Effect of the relative size of two flaws
- Effect of a large number of flaws

Sensitivity to the depth:

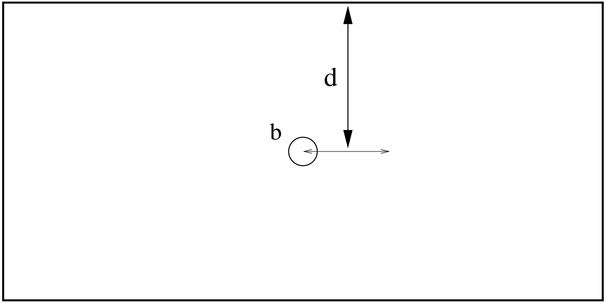

Figure: Mould containing three well-separated flaws having the same radius; $b_1 = B(z_1^*, r*)$, $b_2 = B(z_2^*, r*)$ and $b_3 = B(z_3^*, r*)$

Sensitivity to the depth: The considered error functions:

$$er_1(\delta) = \frac{\|z_h(\delta) - z^*\|}{d}$$
$$er_2(\delta) = \frac{\|z_h(\delta) - z^*\|}{2r^*},$$

where z_h is the computed flaw center.

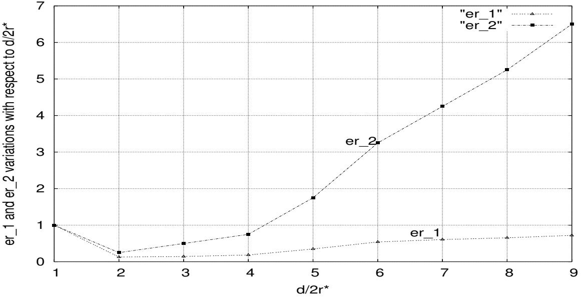

Figure: Variation of the relative errors er_1 and er_2 with respect to the non-dimensional depth δ.

Detection of small flaws locations in moulded objects

Sensitivity to the relative position of two flaws:

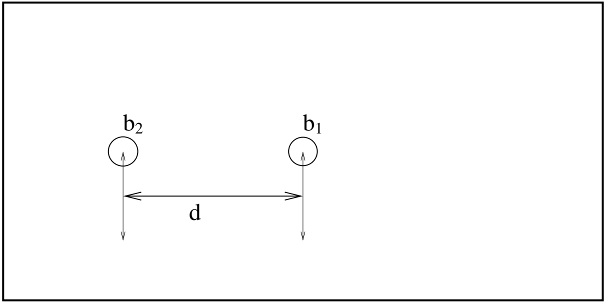

Figure: Mould Ω containing two flaws $b_1 = B(z_1^*, r^*)$ and $b_2 = B(z_2^*, r^*)$ having the same radius r^* and separated by a distance d

Sensitivity to the relative position of two flaws:

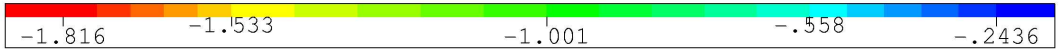

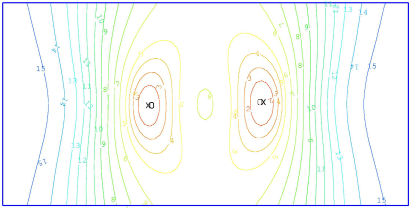

$\rho = 6$

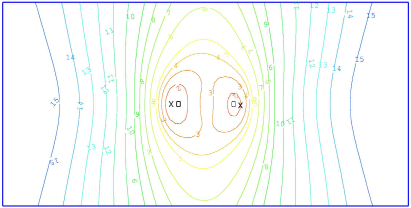

$\rho = 4$

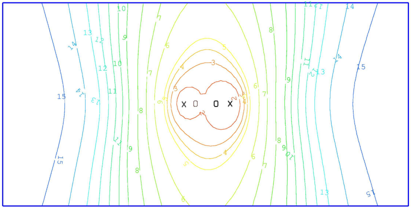

$\rho = 3$

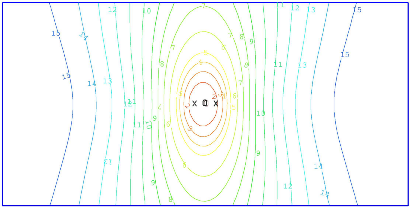

$\rho = 2$

Figure: Isovalues of $\delta\mathcal{J}$ showing the obtained flaw locations ($\times$: exact, o: estimated).

Sensitivity to the relative position of two flaws

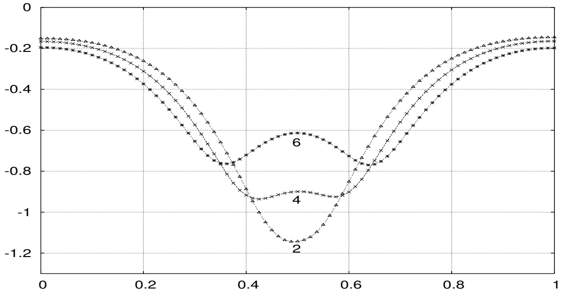

Figure: Values of the topological gradient δj on the line segment crossing the two flaws centers z_1^* and z_2^* for different values of $\rho = d/r^*$; $\rho = 2$, $\rho = 4$ and $\rho = 6$.

Effect of the relative size of two flaws

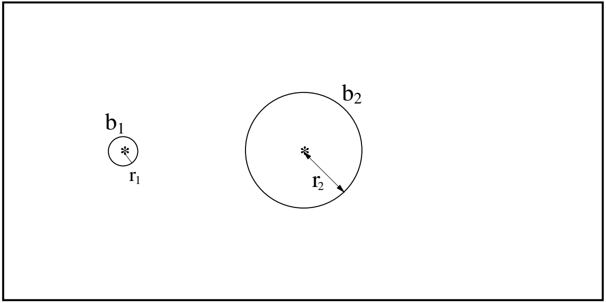

Figure: Mould containing two flaws $b_1 = B(z_1^*, r_1)$ and $b_2 = B(z_2^*, r_2)$ separated by a fixed distance and having a different size (radius) r_1 and r_2

Effect of the relative size of two flaws:

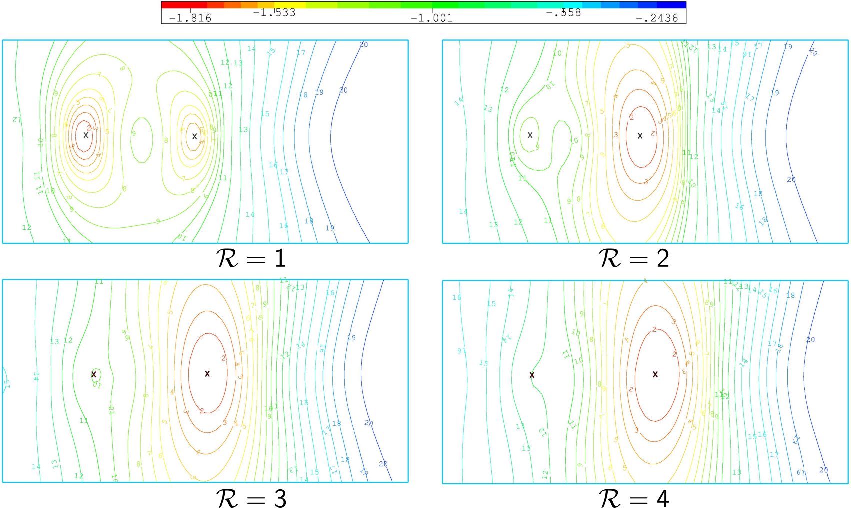

Figure: Isovalues of the topological gradient showing the obtained flaw locations.

Effect of the relative size of two flaws

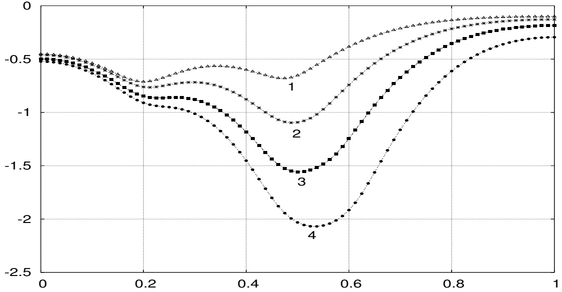

Figure: Values of the topological gradient δj on the line segment crossing the two flaws centers z_1^* and z_2^* for different values of $\mathcal{R} = r_2/r_1$; $\mathcal{R} = 1$, $\mathcal{R} = 2$, $\mathcal{R} = 3$ and $\mathcal{R} = 4$.

Effect of a large number of flaws

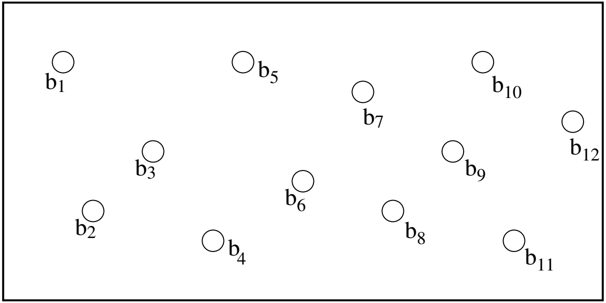

Figure: Large number of flaws having the same size; $b_i = B(z_i^*, r*)$, $1 \leq i \leq 12$.

Detection of small flaws locations in moulded objects

Effect of a large number of flaws:

Using the one-shot algorithm :

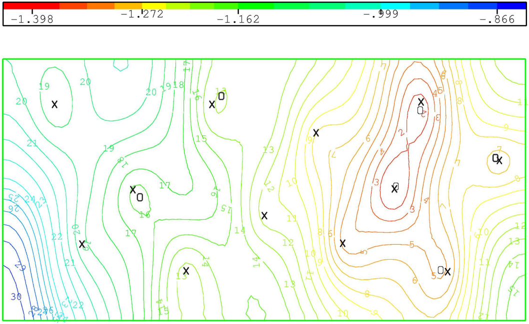

Iterative algorithm:

- Initialization: choose Ω_0 and set $k = 0$.
- Repeat until target is reached:
  - solve the two problems $(\mathcal{P}_N^0)$ and $(\mathcal{P}_D^0)$ in Ω_k,
  - compute the topological sensitivity δj_k in Ω_k,
  - determine the set $H_k = \Big\{ x \in \Omega_k, \quad \delta j_k(x) \le c_k < 0 \Big\}$,
  - determine the detected flaws location $S_k = \cup_{x \in C_k} \{x + 0.02\, B(0,1)\}$, where C_k is the set of the local minima of δj_k in H_k,
  - set $\Omega_{k+1} = \Omega_k \backslash S_k$,
  - $k \longleftarrow k + 1$.

The constant c_k depends on the most negative local minima of δj_k.
In practice we have used $c_k = 0.8\, \delta_{min}$, where δ_{min} is the most negative local minima of $\delta j_k(z)$.

Case of a large number of flaws: using the iterative algorithm

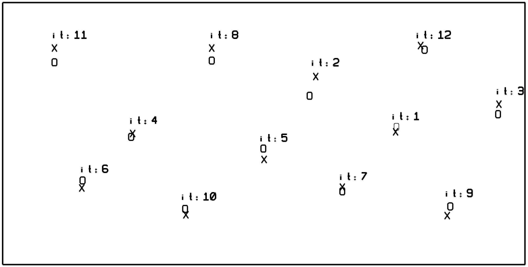

Detection of plasma location in a Tokamak

The Tokamak problem

The Tokamak: The Tokamak is an experimental machine which aims to confine the plasma in a magnetic field to control the nuclear fusion of atoms of mass law. The real-time reconstruction of the plasma magnetic equilibrium in a Tokamak is a key point to access high performance regimes.

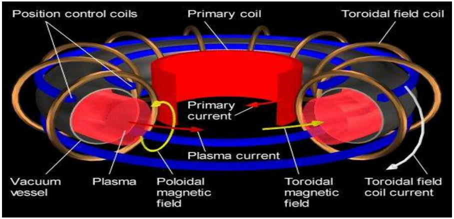

In an axisymmetric configuration, the plasma equilibrium is described by the equation

$$\mathcal{L}\psi = 0 \text{ in } \Omega$$

where $\mathcal{L}$ is the Grad-Shafranov operator

$$\mathcal{L} = -\frac{\partial}{\partial r}\left(\frac{1}{\mu r}\frac{\partial}{\partial r}\right) - \frac{\partial}{\partial z}\left(\frac{1}{\mu r}\frac{\partial}{\partial z}\right)$$

The plasma equilibrium:

We denote by (r, φ, z) the three-dimentional cylindrical coordinates system. Since the tokamak is an axisymmetric troidal device, we may assume that all magnetic quantities do not depend on the troidal angle φ.

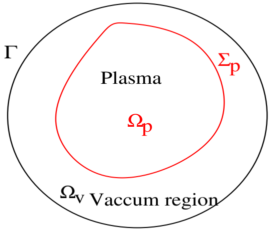

The plasma equilibrium may be studied in any cross section (r, z), named poloidal section.
It is described by the equation

$$L\psi = 0 \text{ in } \Omega_v$$

$-$ Ω_v is the domain included between the tokamak boundary Γ and the plasma boundary Σ, called the vacuum region.
$-$ ψ is the poloidal magnetic flux.
$-$ $\mathcal{L}$ is the Grad-Shafranov operator

$$\mathcal{L} = -\frac{\partial}{\partial r}\left(\frac{1}{\mu r}\frac{\partial}{\partial r}\right) - \frac{\partial}{\partial z}\left(\frac{1}{\mu r}\frac{\partial}{\partial z}\right)$$

The Tokamak problem : We consider here the inverse problem of determining plasma boundary Σ_p location from over-specified boundary data on Γ.

Knowing a complete set of Cauchy data, the poloidal flux ψ satisfies the system

$$\begin{cases} L\psi & = & 0 & \text{in} & \Omega\backslash\overline{\Omega_p}, \\ \dfrac{1}{r}\dfrac{\partial\psi}{\partial n} & = & \Phi & \text{on} & \Gamma, \\ \psi & = & \psi_m & \text{on} & \Gamma, \\ \psi & = & 0 & \text{on} & \Sigma_p. \end{cases}$$

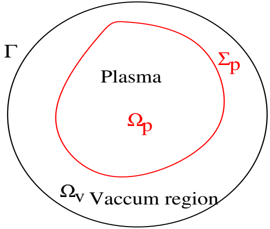

- Ω is the domain limited by the boundary Γ,
- Φ is the magnetic field and ψ_m is the measured poloidal flux on Γ.

In this formulation the domain Ω is unknown since the free plasma boundary Σ_p is unknown. This problem is ill posed in the sense of Hadamard.

Formulation of the problem: In order to determine the unknown plasma boundary Σ_p location we use the Kohn-Vogelius formulation. For any plasma domain Ω_p, we define two forward problems: the first one is associated to the magnetic field Φ (Newmann datum):

$$(\mathcal{P}_N)\left\{\begin{array}{rcl} L\psi_N = & 0 & \text{in } \Omega\backslash\overline{\Omega_p} \\ \dfrac{1}{r}\dfrac{\partial \psi_N}{\partial n} = & \Phi & \text{on } \Gamma \\ \psi_N = & 0 & \text{on } \Sigma_p. \end{array}\right.$$

the second one is associated to the measured poloidal flux ψ_m(Dirichlet datum)

$$(\mathcal{P}_D)\left\{\begin{array}{rcl} L\psi_D = & 0 & \text{in } \Omega\backslash\overline{\Omega_p} \\ \psi_D = & \psi_m & \text{on } \Gamma \\ \psi_D = & 0 & \text{on } \Sigma_p. \end{array}\right.$$

The identification process is based on the minimization of the following energy function

$$\mathcal{K}(\Omega\backslash\overline{\Omega_p}) = \int_{\Omega\backslash\overline{\Omega_p}} \frac{1}{r}|\nabla\psi_D - \nabla\psi_N|^2 \, \mathrm{dx}.$$

The topological sensitivity analysis for the Kohn-Vogelius function:
the Kohn-Vogelius function $\mathcal{K}$ is defined by

$$\mathcal{K}(\Omega \setminus \overline{\omega_\varepsilon}) = \int_{\Omega\setminus\overline{\omega_\varepsilon}} \frac{1}{r} \left|\nabla\psi_N^\varepsilon - \nabla\psi_D^\varepsilon\right|^2 dx,$$

with ψ_N^ε and ψ_D^ε are the solutions to the Neumann and Dirichlet perturbed problems

$$(\mathcal{P}_N^\varepsilon)\begin{cases} L\psi_N^\varepsilon = 0 & \text{in } \Omega\setminus\overline{\omega_\varepsilon} \\ \dfrac{1}{r}\nabla\psi_N^\varepsilon\mathbf{n} = \Phi & \text{on } \Gamma \\ \psi_N^\varepsilon = 0 & \text{on } \partial\omega_\varepsilon, \end{cases} \qquad (\mathcal{P}_D^\varepsilon)\begin{cases} L\psi_D^\varepsilon = 0 & \text{in } \Omega\setminus\overline{\omega_\varepsilon} \\ \psi_D^\varepsilon = \psi_m & \text{on } \Gamma \\ \psi_D^\varepsilon = 0 & \text{on } \partial\omega_\varepsilon. \end{cases}$$

Theorem: The function $\mathcal{K}$ admits the following asymptotic expansion

$$\mathcal{K}(\Omega \setminus \overline{\omega_\varepsilon}) = \mathcal{K}(\Omega) + \frac{-2\pi}{log(\varepsilon)}\frac{1}{x_0}\left[\left|\psi_N^0(X_0)\right|^2 - \left|\psi_D^0(X_0)\right|^2\right] + o(\frac{-1}{log(\varepsilon)}). \qquad (4)$$

One-shot algorithm:

- Compute the topological sensitivity $\delta j(x,y)$, $(x,y) \in \Omega$,
- determine the plasma location by $\Omega_p = \{(x,y) \in \Omega;\ \delta j(x,y) \leq (1-\rho)\, g_{min}\}$ where $g_{min} = \min\limits_{(x,y)\in\Omega} \delta j(x,y)$ and $\rho \in]0,1[$ is a heuristically determined small parameter.

Plasma is likely to be located at zone where the topological gradient δj is negative.

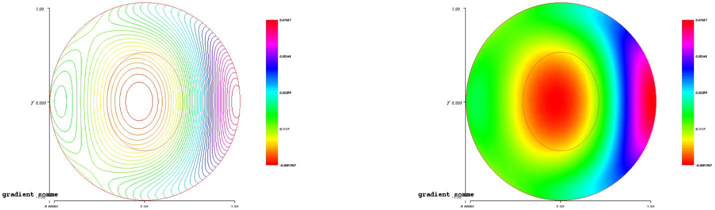

Figure: Isovalues of δj (left) and the obtained (red zone) plasma domain.

Conclusion:

- The theory results are valid for large class of cost functions
- The mathematical analysis is general and can be adapted for ohter PDEs.
- The numerical algorithm is fast: only one iteration.
- The numerical computations are done on a fixed grid.
- Various applications: optimization of injectors location, geometric control of fluid flow, optimal shape design of tubes in a cavity and detection of small flaws locations in moulded objects

Prospects:

- Topological sensitivity analysis for coupled problems.
- Convergence results for the numerical algorithms.
- Optimization of the step length for the iterative process.

Thank you for your attention